

## ARTICLE

**Crystallization, Vitrification, and Gelation of Patchy Colloidal Particles**Shu-jing Liu<sup>a,b</sup>, Jiang-tao Li<sup>a</sup>, Fang Gu<sup>a\*</sup>, Hai-jun Wang<sup>a,c\*</sup>*a. College of Chemistry and Environmental Science, Hebei University, Baoding 071002, China**b. College of Science, Agricultural University of Hebei, Baoding 071001, China**c. Chemical Biology Key Laboratory of Hebei Province, Hebei University, Baoding 071002, China*

(Dated: Received on October 22, 2018; Accepted on November 24, 2018)

We present the phase diagrams for neutral patchy colloidal particles whose surface is decorated by different number of identical patches, where each patch serves as an associating site. The hard-core Lennard-Jones (LJ) potential and associating interaction are incorporated into the free energies of patchy particles in phases of the fluid (F), random close packing (RCP), and face-centered-cubic (FCC) crystal. A rich phase structure of patchy particles with F-F, F-RCP, and F-FCC transitions can be observed. Meanwhile, the sol-gel transition (SGT) characterizing the connectivity of patchy particles is also investigated. It is shown that, depending on the number of patches and associating energy, the F-F transition might be metastable or stable with respect to the F-RCP and F-FCC transitions. Meanwhile, the critical temperatures, critical densities, triple points, and SGT can be significantly regulated by these factors.

**Key words:** Patchy particle, Sol-gel transition, Phase transition, Glass transition**I. INTRODUCTION**

In a recent decade, patchy colloidal particles have attracted intensive attention from many fields. In experiments [1–5], various techniques available for the surface modification have been successfully employed to prepare patchy particles with different shapes and compositions [6–11]. The modified surface of a colloidal particle is usually composed of many functional sub-areas with adjustable areas and chemical components, which are called the patches. This made it possible to regulate the valence (the number of patches) of a patchy particle, and further the energy and range of the interaction between two patchy particles [12–14]. In addition to synthesized patchy particles, some natural biological macromolecules (for instance, globular proteins) can be considered as the patchy particles [15–17], whose anisotropic interaction may be described in terms of effectively attractive patches.

Inspired by relevant experiments, there has been an increasing theoretical effort devoted to aggregation states and phase structures of the patchy particles [18–26]. As a matter of fact, the system of patchy colloidal particles is very complicated because the phase separation, vitrification, and crystallization could take place [27–30]. Meanwhile, colloidal clusters with various sizes and configurations can be generated through the association between patches from different particles. This

kind of connectivity could further result in the sol-gel transition (SGT) or gelation of patchy particles [31–34]. These rich physical phenomena have opened up an active field to address some fundamental questions from different disciplines. As a result, the equilibrium and dynamic properties of patchy particles have been studied [35–38], which mainly include the self-assembly, pattern structures, gas-liquid transition, glass transition, crystallization, transition dynamics, and so forth.

In this work, we pay our attention to several kinds of interesting transitions associated with neutral patchy colloidal particles. An attempt is made to investigate how the associating interaction between patchy particles affects phase structures of the system. The first transition is the fluid-fluid (F-F) transition known as the F-F phase separation, in which fluid phases of low density and high density patchy particles are involved. The second is the fluid-crystal transition, where the face-centered-cubic (FCC) lattice is taken as an example of the crystal phases. The third is the glass transition of patchy particles, where a random close packing (RCP) structure with a density of maximum packing is chosen as the glassy state of patchy particles. The last one is the SGT due to the connectivity of patchy particles, where a colloidal gel network can be formed as a result of the associating interaction. Therefore we will consider F-F, F-FCC, F-RCP transitions as well as SGT occurring in the system of patchy particles.

Nowadays the RCP phase has been identified as the glassy state of matter [39–42]. Hence the F-RCP transition is also referred to the glass transition or vitrification. It should be stressed that the RCP phase is not an equilibrium thermodynamic phase at all, and thus,

---

\* Authors to whom correspondence should be addressed. E-mail: fangu@hbu.edu.cn, whj@hbu.edu.cn

the F-RCP transition is not a true equilibrium phase transition. Strictly speaking, the F-RCP transition belongs to a kinetic transition because the glassy state may have different densities depending on the kinetic conditions. Bearing in mind that the accessible structures at high densities do not necessarily need to be a crystal because a glassy state might take a high density, too. Consequently, the RCP phase or the glassy state is always metastable in nature. Nevertheless, since most of materials can be trapped in the glassy state for a very long time, such a trapped state can be thought of as an intermediate phase between fluid and crystal phases.

It is not a trivial task to study the F-RCP transition. So far almost all proposed theoretical models and simulations on the glass transition require considerable computations concerning the corresponding kinetics and dynamics [43–46]. In this work, the standard theory of phase transitions is employed to treat the F-RCP transition. Specifically, the RCP phase with the density of maximum packing of this kind of structures is used to illustrate several relevant problems, which plays in essence the role of the critical or boundary density in our treatment. Of course, such a treatment needs to be further verified due to the lack of a rigorous theoretical foundation on this issue. The aim is merely to qualitatively capture some common features on the glass transition of patchy particles.

In this work, the expressions of the free energy per particle in fluid, RCP and FCC phases are presented, whereby the phase diagrams can be calculated by the principle of phase equilibria. The phase diagrams describing F-F, F-FCC, and F-RCP transitions are illustrated under various conditions. A significant effect of patch-patch associating interaction on these phase structures is found. Also, we discuss the relationship between glass transition and crystallization of patchy colloidal particles. The interplay between SGT and glass transition are analyzed by combining the SGT together with F-F and F-RCP transitions. We also discuss some drawbacks to be improved.

## II. MODEL AND THEORY

### A. Interactions between two patchy colloid particles

We consider a system consisting of hard-sphere colloidal particles with diameter  $\sigma$ , in which each particle is neutral and possesses  $m$  identical patches decorated uniformly on the surface. For convenience, such colloidal particles are named as the  $A_m$  type of patchy particles. Of particular interest is that there exists an attraction between two patches from different particles under proper distance and orientation. This makes each patch serve as an associating site in such a way that each colloidal particle is capable of bonding with another through the patch-patch attraction. As usual, the hard-sphere repulsion, dispersion, and associating in-

teractions between two patchy particles would be taken into account to present some physical properties of the system.

Let  $r$  be the distance between two patchy colloidal particles, the hard-sphere repulsion potential  $V_{\text{HS}}(r)$  between them is infinity for  $r < \sigma$ , and zero otherwise. As is usually the case, the interparticle dispersion interaction can be given by the conventional Lennard-Jones (LJ) potential:

$$V_{\text{DIS}}(r) = 4\varepsilon_{\text{LJ}} \left[ \left( \frac{\sigma}{r} \right)^{12} - \left( \frac{\sigma}{r} \right)^6 \right], \quad r \geq \sigma \quad (1)$$

where  $\varepsilon_{\text{LJ}}$  measures the minimum of the LJ potential, which is also known as the dispersion energy.

In the system of patchy particles, the most important interaction is the interparticle association resulting from the patch-patch attraction. Experimentally, this kind of association can be effectively regulated by both the number of patches and the features of patches such as area, geometry, and chemical compositions. Theoretically, a simple square-well (SW) potential can be used to model the associating interaction of a pair of patches from distinct particles, which would specify the association energy and attraction range as well as the separation and orientation of two patches [47].

However, it is not easy to deal rigidly with an interparticle interaction with the orientations. A customary treatment is to take advantage of an effective interaction potential with only the distance dependence. To this end, an angle-average of the used SW potential over all orientations of two particles has to be performed to obtain a desired associating potential. Such an average can be undertaken according to the proposal given by Wertheim [48]. As we have done in a previous study [49], this yields the following two-body associating (ASS) potential:

$$V_{\text{ASS}}(r) = -m\varepsilon_{\text{ASS}}S(r, \lambda), \quad \sigma \leq r \leq \sigma + \lambda \quad (2)$$

where  $\varepsilon_{\text{ASS}}$  measures the association energy, and  $\lambda$  denotes the patch-patch attraction range over which the patch-patch attraction is forbidden. Meanwhile, the degeneracy of the association pairs has been taken into account, and the function  $S(r, \lambda)$  takes the form:

$$S(r, \lambda) = \frac{(\lambda + \sigma - r)^2(2\lambda - \sigma + r)}{6\sigma^2r} \quad (3)$$

Throughout this work,  $\lambda=0.12\sigma$  has been used to avoid multiple associations of a patch following the proposal of Sciortino and coworkers [50, 51]. This guarantees that each site is engaged at most in one pair of association.

### B. Free energy per patchy particle in the fluid phase

The phase equilibria can be investigated in a straightforward manner when the free energies of particles in

different phases are figured out. In practice, it is more convenient to use the free energy per particle to predict the phase equilibria, instead of the free energy. For patchy colloidal particles in the fluid phase, the corresponding free energy can be derived under the framework of thermodynamic perturbation theory [52]. According to the above-mentioned interparticle interactions, the free energy per particle in the fluid phase of number density  $\rho$  can be written as:

$$f^F(\rho) = f_{ID}^F(\rho) + f_{HS}^F(\rho) + f_{DIS}^F(\rho) + f_{ASS}^F(\rho) \quad (4)$$

where the superscript ‘‘F’’ is inferred to the fluid phase of patchy particles, and  $f_{ID}^F(\rho)$ ,  $f_{HS}^F(\rho)$ ,  $f_{DIS}^F(\rho)$ , and  $f_{ASS}^F(\rho)$  denote contributions from the ideal part, hard sphere repulsion, dispersion, and associating interactions, respectively.

In Eq.(4),  $f_{ID}^F(\rho)$  is exactly known as  $f_{ID}^F(\rho) = \beta^{-1}[\ln(\rho\Lambda^3) - 1]$  with the de Broglie thermal wavelength  $\Lambda$ , while  $\beta^{-1} = k_B T$  is the product of the Boltzmann constant  $k_B$  and absolute temperature  $T$ . The hard sphere part  $f_{HS}^F(\rho)$  can be obtained from the Carnahan-Starling equation [53]:

$$\beta f_{HS}^F(\rho) = \eta \frac{4 - 3\eta}{(1 - \eta)^2} \quad (5)$$

in which  $\eta = \frac{\pi}{6} \rho \sigma^3$  is the packing fraction of colloidal particles in the bulk phase. The dispersion free energy per particle  $f_{DIS}^F(\rho)$  can be derived from the LJ potential in Eq.(1),

$$\beta f_{DIS}^F(\rho) = -\frac{32}{3} \eta \beta \varepsilon_{LJ} \quad (6)$$

Furthermore, with the aid of statistical association fluid theory [50–52], the association free energy per particle  $f_{ASS}^F(\rho)$  can be given by:

$$\beta f_{ASS}^F(\rho) = m \left[ \ln(1 - p) + \frac{p}{2} \right] \quad (7)$$

where  $p$  is defined as the associated fraction of patches, which is determined by the following mass action law for describing the associating interaction between two patches [51, 54]:

$$\frac{p}{m(1 - p)^2} = \rho V_b g_{HS}(\rho) [\exp(\beta \varepsilon_{ASS}) - 1] \quad (8)$$

where  $V_b$  is the patch-patch associating volume,  $g_{HS}(\rho)$  is the radial distribution function of hard sphere fluid at density  $\rho$ . In this work,  $V_b = 0.332 \times 10^{-3} \sigma^3$  has been employed to satisfy the requirement of the single bond per patch on associating [51]. More strictly, a modified  $g_{HS}(\rho)$  [55] should be used to take into account the effect of patch-patch attraction range  $\lambda$ . Note that  $\lambda = 0.12\sigma$  has been adopted to avoid multiple associations of a patch. In such a situation, little difference between values of  $p$  evaluated using  $g_{HS}(\rho)$  and its modified form can be observed, and the corresponding influence on the phase diagrams is negligible. In this sense,  $g_{HS}(\rho)$  is a good approximation and can be used in Eq.(8).

### C. Free energy per patchy particle in FCC and RCP phases

For brevity, hereafter some physical quantities with the superscript ‘‘S’’ would imply that they correspond to the FCC or RCP phases. In this way, the free energy per particle can be expressed as a sum of four terms:

$$f^S(\rho) = f_{ID}^S(\rho) + f_{HS}^S(\rho) + f_{DIS}^S(\rho) + f_{ASS}^S(\rho) \quad (9)$$

where  $f_{ID}^S(\rho)$ ,  $f_{HS}^S(\rho)$ ,  $f_{DIS}^S(\rho)$ , and  $f_{ASS}^S(\rho)$  are the contributions of the ideal part, hard core repulsion, dispersion, and associating interactions to the free energy per particle, respectively. In the equation,  $f_{DIS}^S(\rho)$  and  $f_{ASS}^S(\rho)$  have been arranged to be the same as  $f_{DIS}^F(\rho)$  and  $f_{ASS}^F(\rho)$ .

On the basis of the cell theory [42],  $f_{HS}^S(\rho)$  can be written as:

$$\beta f_{HS}^S(\rho) = 3 \ln \left\{ 2 \left[ 1 - \left( \frac{\rho}{\rho_{cp}} \right)^{1/3} \right] \right\} \quad (10)$$

in which  $\rho_{cp}$  is the density of maximum packing (also the closest packing) in the phase of interest. For instance,  $\rho_{cp}^{FCC} \sigma^3 = \sqrt{2}$  in a FCC lattice, and  $\rho_{cp}^{RCP} \sigma^3 = 1.203$  in a RCP phase. Furthermore, making use of the dispersion interaction given in Eq.(1), one can obtain the corresponding dispersion free energy per particle:

$$\beta f_{DIS}^S(\rho) = 2\varepsilon_{LJ} \left[ \left( \frac{\rho}{\rho_{cp}} \right)^4 M_{12} - \left( \frac{\rho}{\rho_{cp}} \right)^2 M_6 \right] \quad (11)$$

where  $M_6$  and  $M_{12}$  denote the Madelung constants [56] resulting from attraction and repulsion interactions between particles, respectively.

For simple cubic (SC), body-centered-cubic (BCC), and FCC lattices, Madelung constants  $M_6$  and  $M_{12}$  are available in Ref.[56]. From  $M_6$  and  $M_{12}$  for SC, BCC, and FCC lattices given in Table I, an obvious density dependence of  $M_6$  and  $M_{12}$  can be found. Note that the positions of particles in the RCP phase are randomly distributed. As such, neither explicit expressions nor relevant data for  $M_6$  and  $M_{12}$  in the RCP phase are available due to such a randomness of positions of particles.

Nonetheless, one can find that within the framework of the cell theory, the free volume of a particle in a solid phase is closely related to the density of maximum packing  $\rho_{cp}$ , so do the Madelung constants  $M_6$  and  $M_{12}$ . Inspired by this kind of density dependence, we intuitively think that this fact holds true in the RCP phase. Consequently, an exponential fitting by considering  $\rho_{cp}^{RCP} \sigma^3 = 1.203$  enables us to find that  $M_6 = 10.78$  and  $M_{12} = 7.76$  in a RCP lattice, as the crosses shown in FIG. 1. The fitting is expected to validate in a RCP lattice so that the fitted Madelung constants can be employed to present some relevant thermodynamic properties. For convenience,  $M_6$  and  $M_{12}$  for SC, BCC, FCC, and RCP phases are listed in Table I.

TABLE I Madelung constants  $M_6$  and  $M_{12}$  for SC, BCC, FCC, and RCP phases. For SC, BCC, and FCC phases, the values are taken from Ref.[56]; and for the RCP phase, the values are obtained by an exponential fitting in this work.

	SC	BCC	FCC	RCP
$\rho_{cp}\sigma^3$	1.00	$3\sqrt{3}/4$	$\sqrt{2}$	1.203
$M_6$	8.40	12.25	14.45	10.78
$M_{12}$	6.20	9.11	12.13	7.76

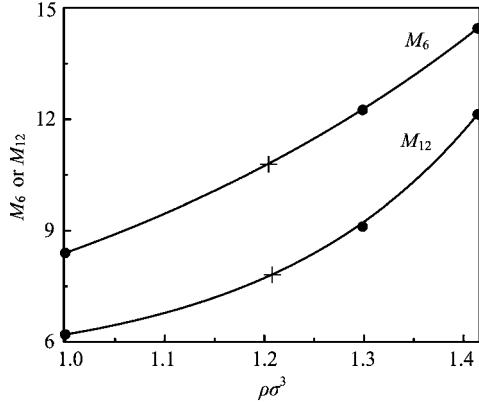


FIG. 1 Fitted curves of Madelung constants  $M_6$  and  $M_{12}$  for SC, BCC, FCC, and RCP phases, where the crosses correspond to the RCP phase.

#### D. Phase equilibria of a patchy colloid

Once the expressions of the free energy per particle for fluid, RCP, and FCC phases of patchy particles are known, the chemical potential  $\mu$  and pressure  $P$  can be obtained by the standard thermodynamic relationships:

$$\mu = f + \rho \left( \frac{\partial f}{\partial \rho} \right) \quad (12)$$

$$P = \rho^2 \left( \frac{\partial f}{\partial \rho} \right) \quad (13)$$

As a phase  $\alpha$  is in equilibrium with a phase  $\gamma$ , the phase diagram of the patchy colloidal particles can be calculated by solving the following coexistence equations:

$$\mu_\alpha(\rho_\alpha, T) = \mu_\gamma(\rho_\gamma, T) \quad (14)$$

$$P_\alpha(\rho_\alpha, T) = P_\gamma(\rho_\gamma, T) \quad (15)$$

where  $\mu_X(\rho_X, T)$  and  $P_X(\rho_X, T)$  denote the chemical potential and pressure of particles in the phase  $X$  at density  $\rho_X$  and temperature  $T$ , respectively. The quantities  $\mu_X(\rho_X, T)$  and  $P_X(\rho_X, T)$  also depend implicitly on the number of patches, association energy, and dispersion energy. Clearly, one can find how the associating interaction regulates the phase structures of the patchy particles when the phase diagrams are illustrated under various conditions.

Then we are devoted to investigating the effect of these factors on the F-F, F-FCC, and F-RCP transitions, as well as SGT. For this purpose, it is more

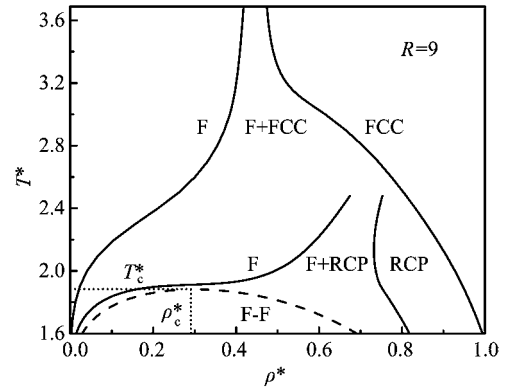


FIG. 2  $T^*$ - $\rho^*$  phase diagrams of F-F, F-RCP, and F-FCC transitions in  $A_4$  type of patchy particles at  $R=9$ , where  $T_c^*$  and  $\rho_c^*$  denote the critical temperature and critical density for the F-F binodal.

convenient to use the reduced temperature defined by  $T^* = k_B T / \epsilon_{LJ}$  and a reduced density defined by  $\rho^* = \rho \sigma^3$  to present relevant discussions. Moreover, the ratio of association energy to dispersion energy defined by  $R = \epsilon_{ASS} / \epsilon_{LJ}$  is also introduced, and thus different values of  $R$  reflect the change of the association energy. When all these parameters are specified, one can present the phase diagrams of patchy colloidal particles, whereby the influences of these factors can be analyzed.

### III. CRYSTALLIZATION AND GLASS TRANSITION OF PATCHY PARTICLES

To illustrate phase diagrams of patchy colloidal particles under various conditions, we would firstly focus on the F-F, F-FCC, and F-RCP transitions. Here F-F transition is referred to the transition between a gas-like low density fluid and a liquid-like high density fluid. Note that the F-FCC and F-RCP transitions are associated with the crystallization (fluid-crystal transition) and vitrification (glass transition), respectively. An attempt is made to reveal the influence of both the number of patches and association energy on the phase structures of patchy particles.

For easy of presentation, we firstly present the  $T^*$ - $\rho^*$  phase diagram concerning F-F, F-RCP, and F-FCC transitions for  $A_4$  type of patchy particles at  $R=9$ , as illustrated in FIG. 2. It is shown that both the liquid-like fluid phase and the RCP phase are metastable with respect to the FCC phase, where the critical point of the F-F binodal is characterized by  $T_c^*$  and  $\rho_c^*$ . Obviously, the fluid, RCP and FCC phases display distinct phase behavior in phase region and binodal. Furthermore, upon changing the number of patches and parameter  $R$ , some detailed influences of these factors on F-F, F-RCP, and F-FCC transitions can be observed. Interestingly, the responses of F-F and F-RCP transitions, and F-F and F-FCC transitions to the number of patches

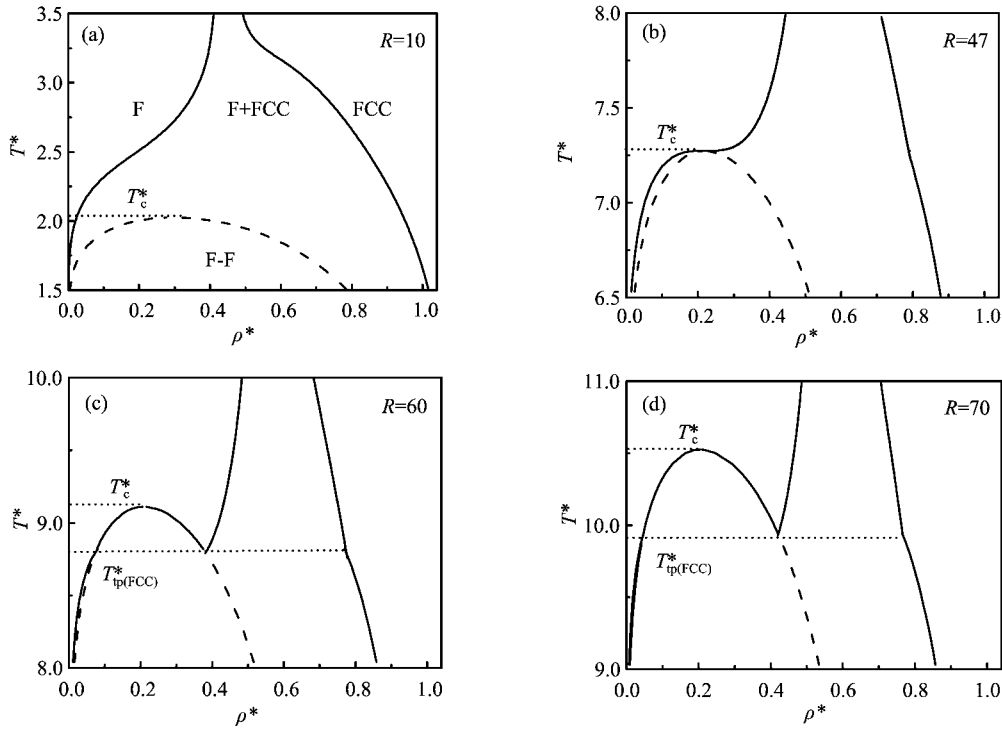


FIG. 3  $T^*$ - $\rho^*$  phase diagrams of F-F and F-FCC transitions in  $A_4$  type of patchy particles at different  $R$ : (a)  $R=10$ , (b)  $R=47$ , (c)  $R=60$ , (d)  $R=70$ ;  $T_{\text{tp(FCC)}}^*$  denotes the triple point associated with F-F and F-FCC transitions. For clarity, the phase regions are only labeled in (a).

and parameter  $R$  are also different from each other, as presented below.

#### A. Phase diagrams for F-F and F-FCC transitions

FIG. 3 presents the  $T^*$ - $\rho^*$  phase diagrams including F-F and F-FCC transitions for  $A_4$  type of patchy particles under different association energy indicated by different  $R$ . Clearly, the liquid-like fluid phase at a relatively low  $R$  ( $R=10$ ) is metastable with respect to FCC phase. Upon increasing  $R$ , the liquid-like fluid phase undergoes a critical metastable state ( $R=47$ ), and eventually becomes stable at a relatively high  $R$  ( $R=60$ ). This can be found by the appearance of a triple point defined by the temperature of  $T_{\text{tp(FCC)}}^*$ , at which the gas-like and liquid-like fluids, and FCC-crystal can coexist in the system. FIG. 3(b) shows the critical metastable state ( $R=47$ ) corresponding to the case  $T_c^*=T_{\text{tp(FCC)}}^*$ . All the results in FIG. 3 indicated the key role of the association energy playing in the crystallization of patchy colloidal particles.

As is well known, the associating interaction between two patchy particles is jointly determined by both the association energy and the number of patches. In a previous study, the suppression of the gas-liquid phase separation upon decreasing the valence was presented [50]. As such, the influence of the number of patches on the crystallization of patchy particles is also note-

worthy. FIG. 3 has shown that both  $T_c^*$  and  $T_{\text{tp(FCC)}}^*$  are closely related to the association energy, whereby one can infer an obvious effect of the number of patches  $m$ . To illustrate this, we have investigated the changes of  $T_c^*$  and  $T_{\text{tp(FCC)}}^*$  at different  $m$  and  $R$ , as shown in FIG. 4.

Clearly,  $T_c^*$  increases monotonically with an increase in  $R$  as  $m$  is fixed, and also increases with an increase in  $m$  as  $R$  is fixed. Meanwhile, one can find from FIG. 3(b) that there always exists a special temperature at which  $T_c^*$  equals to  $T_{\text{tp(FCC)}}^*$ . Such a special temperature corresponds to the critical metastable-stable transition, which means that a well-defined triple point would appear in the system. Therefore it can be called the critical triple point associated with F-F and F-FCC transitions. Above the critical triple point the system allows gas-like and liquid-like fluids to coexist with FCC-crystal, while below which the liquid-like fluid phases would be metastable with respect to the FCC-crystal. Furthermore, one can observe that the appearance of the critical triple point at a larger  $m$  always requires a larger  $R$ , as indicated by the short dot line in FIG. 4. This manifests that the stronger the associating interaction, the higher the critical triple point. On the basis of FIG. 3 and FIG. 4, one can conclude that the associating interaction between patchy particles is indeed predominant in studying the phase equilibria of the patchy colloid.

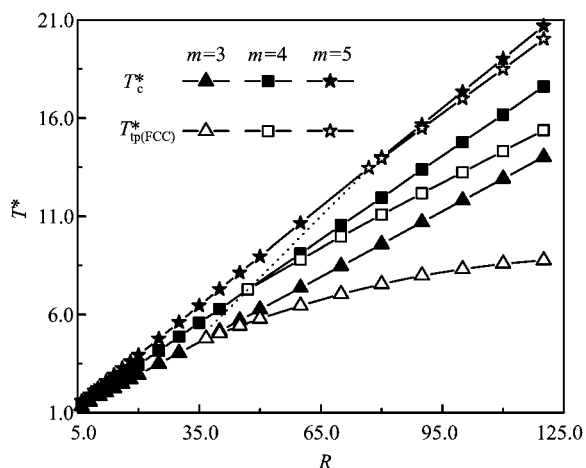


FIG. 4  $T_c^*$  and  $T_{\text{tp(FCC)}}^*$  for F-F and F-FCC transitions at different  $m$  and  $R$ , where the short dot line denotes the critical triple point.

### B. Phase diagrams for F-F and F-RCP transitions

F-RCP transition is closely related to the glass transition or vitrification since the glassy state has the same structures as the RCP phase. In a glass-forming system, the effect of kinetic factors such as the annealed temperature and cooling rate is very significant. Consequently, some typical physical quantities such as viscosity and thermal properties depend strongly on the kinetic process. For patchy colloidal particles, some investigations have proposed that the formation of colloidal glass is induced by the broken ergodicity or arrested dynamics [57–62]. So far such an issue has attracted an increasing interest from both experimental and theoretical viewpoints.

Now, the F-RCP transition would be studied by the standard theory of phase transitions, and an attempt is merely made to explain qualitatively the interplay among fluid, glass and crystal phases. For this purpose, the density of maximum packing of the glassy state ( $\rho_{\text{cp}}^{\text{RCP}*}=1.203$ ) would be used. This means that as  $\rho^* \geq 1.203$ , the RCP phase would be no longer stable with respect to the fluid phase. It is therefore only in a phenomenological sense that such a treatment holds true due to the fact that the glassy state is not a well-defined equilibrium thermodynamic phase.

FIG. 5 shows the  $T^*-\rho^*$  phase diagrams for F-F and F-RCP transitions in  $A_4$  type of patchy particles at different  $R$ . Compared with the F-RCP transition, it has been explicitly illustrated that on increasing  $R$ , the liquid-like fluid phase changes from a metastable one to a stable one. As shown in FIG. 5(b), there still exists a special temperature indicated by  $T_c^*=T_{\text{tp(RCP)}}^*$  at  $R=9.68$ , at which the liquid-like fluid phase becomes critical metastable with respect to the RCP phase. In analogy to the discussion on the F-F and F-FCC transitions, such a special temperature could be called a phe-

nomenological critical triple point concerning the gas-like, liquid-like, and RCP phases.

It can be observed that  $T_c^*$  and  $T_{\text{tp(RCP)}}^*$  always increase with  $R$ . This suggests that a larger association energy leads to higher transition temperatures  $T_c^*$  and  $T_{\text{tp(RCP)}}^*$ . Moreover, when  $T_c^* < T_{\text{tp(RCP)}}^*$ , the liquid-like fluid phase would be metastable compared with the RCP phase. On the contrary, when  $T_c^* > T_{\text{tp(RCP)}}^*$ , the gas-like and liquid-like fluid phases as well as the RCP phase (glassy state) would be stable and could coexist with each other in the system. Of course, it is inevitable that, depending on the kinetic and dynamic conditions, the system would further evolve towards the most stable crystal phase.

Furthermore, the effect of the number of patches on  $T_c^*$  and  $T_{\text{tp(RCP)}}^*$  is also presented, as shown in FIG. 6. Clearly, both  $T_c^*$  and  $T_{\text{tp(RCP)}}^*$  at a fixed  $m$  increase monotonically with an increase in  $R$ , and at a fixed  $R$  they also increase with increasing  $m$ . In this sense, the effect of the number of patches on F-F and F-RCP transitions is similar to that on the F-F and F-FCC transitions. However, unlike the dependence of the critical  $T_{\text{tp(FCC)}}^*$  on  $m$  and  $R$ , the critical  $T_{\text{tp(RCP)}}^*$  at a larger  $m$  needs a smaller  $R$ . This kind of difference can be observed by comparing the short dot line in FIG. 4 with the short dot line in FIG. 6. Combining the results in FIG. 5 and FIG. 6, a significant effect of the associating interaction between patchy particles on the glass transition can be easily observed.

### C. Nucleation and growth in glass transition and crystallization

The glassy state of matter is always metastable with respect to the FCC-crystal state. In experiments, depending on thermodynamic conditions and kinematic factors of the system, the timescale for the glass-crystal transformation can even change by many orders of magnitude. This made the relationship between vitrification and crystallization be a fascinating issue for a few decades. It is well known that one-step nucleation is the most frequently encountered situation in crystallization. However, as pointed out by some studies [63–67], it is also possible that a system undergoes a two-step nucleation process. In essence, besides thermodynamic and dynamic conditions, the one-step or two-step mechanisms of nucleation should be mainly determined by the interparticle interactions.

It is of particular interest to study whether the present system of patchy particles can serve as a model system to illustrate two types of possible mechanisms for nucleation in crystallization. As already presented above, the F-RCP and F-FCC transitions depend strongly on the associating interaction between patchy particles. Also, it is easy to find that the RCP phase is indeed metastable compared with the FCC

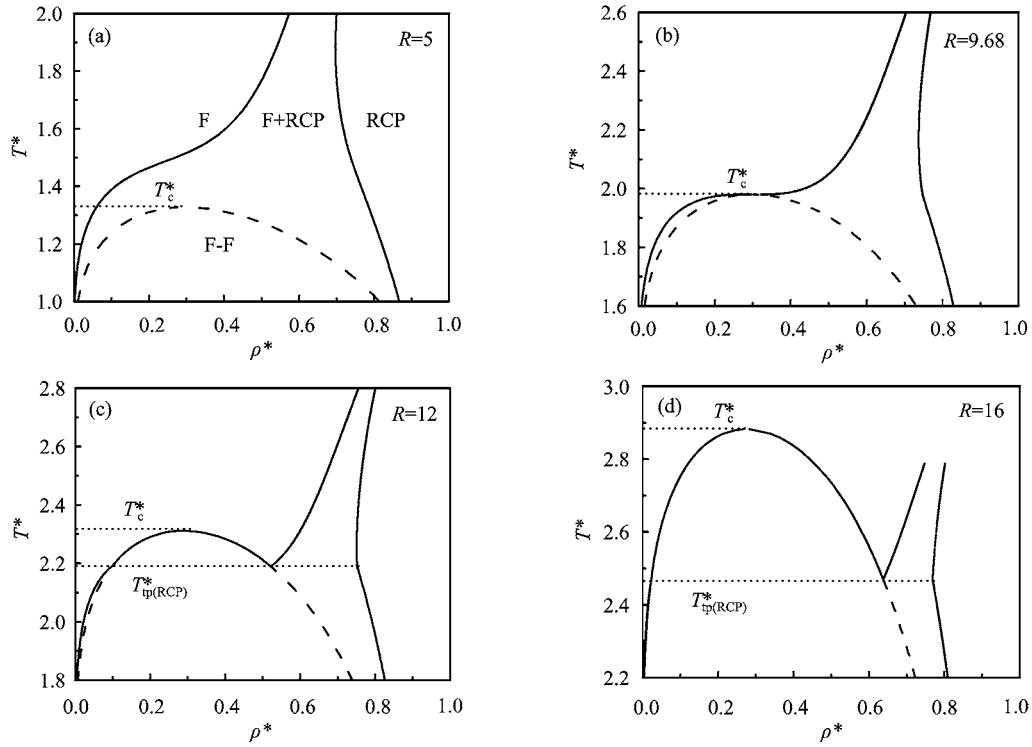


FIG. 5  $T^*$ - $\rho^*$  phase diagrams of F-F and F-RCP transitions in  $A_4$  type of patchy particles at different  $R$ : (a)  $R=5$ , (b)  $R=9.68$ , (c)  $R=12$ , (d)  $R=16$ ;  $T_{\text{tp(RCP)}}^*$  denotes the triple point of fluid and RCP phases. For clarity, the phase regions are only labeled in panel (a).

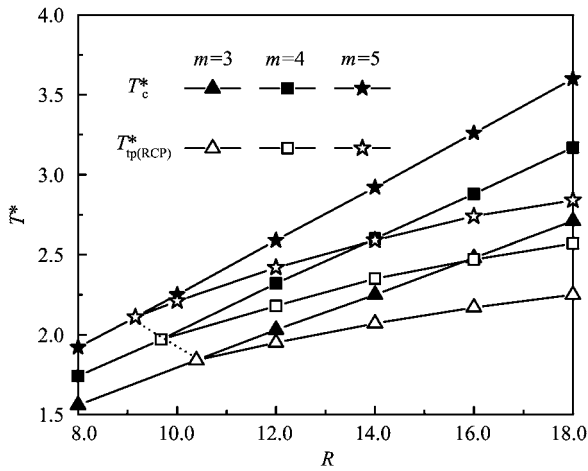


FIG. 6  $T_c^*$  and  $T_{\text{tp(RCP)}}^*$  for F-F and F-RCP transitions at different  $m$  and  $R$ , where the short dot line denotes the critical triple point.

phase under various conditions. However, the liquid-like fluid phase is not always the case. To discuss the possible nucleation mechanisms, the phase diagrams including F-F, F-RCP, and F-FCC transitions have been illustrated in FIG. 7.

FIG. 7(a) shows the phase diagram where the liquid-like fluid phase is metastable with respect to the RCP phase, but it is no longer metastable in FIG. 7(b). In

the figure,  $T_G^*$  denotes the critical temperature at which the RCP phase appears, and above which no F-RCP transition can be obtained. This means that above  $T_G^*$  the crystallization is subjected to the one-step nucleation mechanism. In such a process, the FCC crystal is in favor of a loosely packed lattice corresponding to an expanded structure of FCC lattice. When the quench temperature below  $T_c^*$ , the crystallization would be subjected to a two-step nucleation mechanism. In the two-step nucleation process, the crystallization from the gas-like fluid to the FCC-crystal would undergo a free energy barrier resulting from the liquid-like fluid phase.

Note that both liquid-like fluid associated with F-F transition and RCP phase are always metastable with respect to FCC phase in FIG. 7. This implies that when  $T^* < T_G^*$ , both the one-step and two-step nucleation processes could undergo the glass transition, thereby leading the crystallization to be a complicated process. In the case of  $T^* < T_G^*$ , there exist the high-density fluid and RCP phases between the low-density fluid and FCC phases. This indicates that vitrification would serve as a transition state between the high density fluid and FCC-crystal, and also provide an extra free energy barrier.

Physically, the diffusion of colloid particles at a high temperature is so fast that they can adopt the configurations to crystallize by taking a crystal-like cluster as a nucleation. On the contrary, colloidal particles at a low

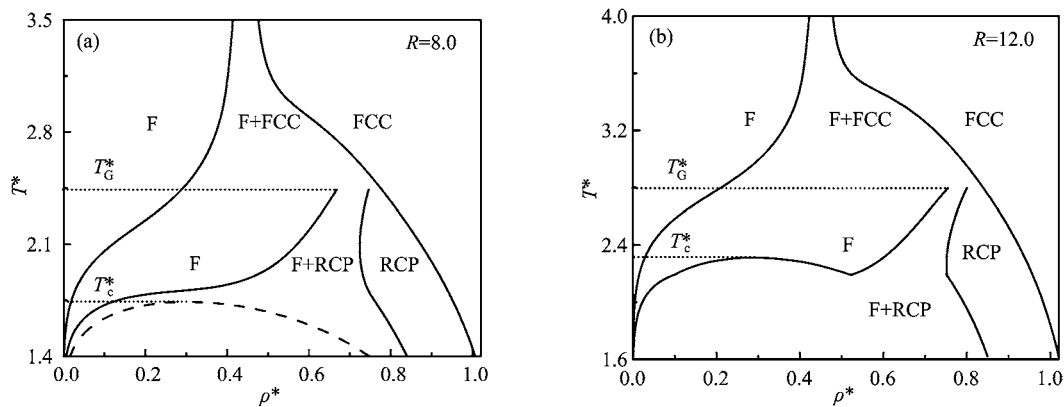


FIG. 7  $T^*$ - $\rho^*$  phase diagrams of the  $A_4$  type of patchy particles for  $R=8.0$  (a) and  $R=12.0$  (b), where  $T_G^*$  is the critical temperature at which the RCP phase appears.

temperature slow down their diffusion in momentum space. Meanwhile, the interparticle association also reduces their possible configurations. This greatly limits the reorganization of particles in phase space, thereby breaking the ergodicity. When the temperature is so low that the diffusion of particles is frozen, the system would be kinematically arrested. In this sense the formation of the glassy state ascribes to the arrested dynamics. As a consequence of the phase separation, patchy particles will firstly form clusters of high densities, and then these clusters evolve into the disordered RCP phase. The subsequent development from the RCP phase would be determined by the dynamic conditions of the system. Such a process may need a considerable time and display a complicated dynamic behavior, which is beyond the scope of this article.

#### IV. SOL-GEL TRANSITION AND GLASS TRANSITION

The connectivity of patchy colloidal particles can give rise to the formation of a large number of colloidal clusters with various sizes and configurations. Under appropriate conditions, the weight-average molecular weight of these clusters could be infinity, which signals the gelation in the system. This means that the colloidal gel would appear as long as the associated fraction of patches  $p$  approaches a critical value  $p_c$ . Such a process is called the SGT with  $p_c$  as its percolation threshold.

Unlike a chemical gel with a considerable lifetime, the present colloidal gel at the beginning of SGT is always composed of transient clusters with a very short lifetime. This is due to the fact that the patch-patch attraction is usually very weak compared with a covalent bond, and thus no stable colloidal gel can be generated as the system is just above the percolation threshold. In the present system, the formation of a colloidal gel is often accompanied with the phase separation process and even the glass transition. As such, the SGT, F-F, and F-RCP transitions in the system of patchy particles

have attracted an increasing interest.

Motivated by such a topic, we will focus on the relationship among SGT, F-F, and F-RCP transitions. To this end, we will firstly give the gelation criteria (gel point)  $p_c$  according to the classical gelation theory [68]. The classical gelation theory often adopts two assumptions. The former is the assumption of equal reactivity of functional groups, and the latter is that no intramolecular reactions occur in the sol phase. In this way, the gel point of a large number of polymerization systems can be obtained in a straightforward manner. For an  $A_m$  type of patchy particles under these assumptions, the gel point  $p_c$  can be expressed as  $p_c=1/(m-1)$  [68]. The combination of  $p_c$  and the mass action law in Eq.(8) yields:

$$\rho V_b g_{HS}(\rho) [\exp(\beta \varepsilon_{ASS}) - 1] = \frac{m-1}{m(m-2)^2} \quad (16)$$

which enables us to obtain the phase diagram of SGT, where the  $T^*$ - $\rho^*$  plane would be divided into sol and gel regions separated from each other by the SGT line.

In view of the weakness of the patch-patch association, the present SGT line only indicates the percolation threshold of patchy particles, and is by no means the gel line. In general, the gel line always means that an infinite and stable spanning cluster can be found in the system. Obviously, a stable gel could be formed by either quenching down a very low temperature or increasing the associated fraction  $p$  up to a large value. By doing so, the former increases the patch-patch association strength due to the low temperature (a non-equilibrium route), whereas the latter leads the gel cluster to a loop-rich network structure (the cooperation of a large number of loops in a network would enhance the lifetime of a gel).

FIG. 8 shows the  $T^*$ - $\rho^*$  phase diagram of the SGT together with the F-F transition at a fixed  $R=15$  and different  $m$ . It can be found that there was always intersection of F-F binodal and SGT line characterized by  $T_{SG}^*$  and  $\rho_{SG}^*$ . This indicates that when  $T^* < T_{SG}^*$ ,

the SGT would be covered by the spinodal decomposition and further nucleation resulting from the phase separation. In this way, the gelation becomes rather complicated because the gel state would be unstable until it approaches the boundary of F-F transition. It is therefore possible that the physical gelation is identified as the first order thermodynamic phase transition. Conversely, in the case of  $T^* > T_{SG}^*$ , sol and gel phases would not be relevant to F-F transition. Accordingly, the gel is composed of many transient large-sized clusters, which is entirely different from those clusters in the sol phase.

Interestingly, an obvious shrinking of the coexistence region of low- and high-density fluid phases can be observed upon decreasing the number of patches. This agrees with the findings of Bianchi and coworkers [50], and also manifests that F-F transition can be effectively regulated by the number of patches. In addition, in FIG. 8,  $T_{SG}^*$  and  $T_c^*$ ,  $\rho_{SG}^*$  and  $\rho_c^*$  also show their dependence on the valence and association energy ( $m$  and  $R$ ). To illustrate this situation more specifically, the plots of these quantities against  $m$  at different  $R$  have been presented, as shown in FIG. 9.

Clearly,  $T_{SG}^*$  and  $T_c^*$  increase with both  $f$  and  $R$ , but the variations of  $\rho_{SG}^*$  and  $\rho_c^*$  are more or less complicated: (i)  $\rho_c^*$  increases monotonically with  $m$ , but its change against  $R$  is related to  $m$ . Below a certain value of  $m$  (say,  $m=7$ ), the more the  $R$ , the lower the  $\rho_c^*$  is. While above this value, the dependence of  $\rho_c^*$  on  $R$  becomes not obvious. (ii)  $\rho_{SG}^*$  always decreases monotonically with increasing  $R$ , but its dependence on  $m$  is not the case. Upon increasing  $m$ ,  $\rho_{SG}^*$  firstly decreases, and then increases gradually. (iii) The situation of  $\rho_c^*$  less than  $\rho_{SG}^*$  is possible only when the associating interaction is weak, *i.e.*, a low valence  $m$  and small  $R$ . These results indicate that the associating interaction between patchy particles indeed plays an important role in the SGT.

It is well known that a gel phase is usually composed of some disordered clusters, which can be fractal or network structures. Meanwhile, the glassy state is also disordered and can be formed when a high density fluid undergoes a quench process. One can infer that the disordered gel phase may be related to the glassy state, and thus questions arise naturally: under what conditions could a gel phase be thought of as a glassy state? can we get some possible clues through the phase diagram including SGT, F-F, and F-RCP transitions?

FIG. 10 illustrates the corresponding diagrams at a fixed  $m$  for different  $R$ . It can be observed that at a low  $R$ , the SGT line would be inside the coexisting region of the liquid-like fluid and the RCP phases. Upon increasing  $R$ , the SGT line is gradually far from the coexisting region. Clearly, the proximity of the SGT line to the F-RCP coexist region depends obviously on the parameter  $R$ , and hence the patch-patch association energy. More specifically, the smaller the parameter  $R$ , the larger the proximity is. This means again that the

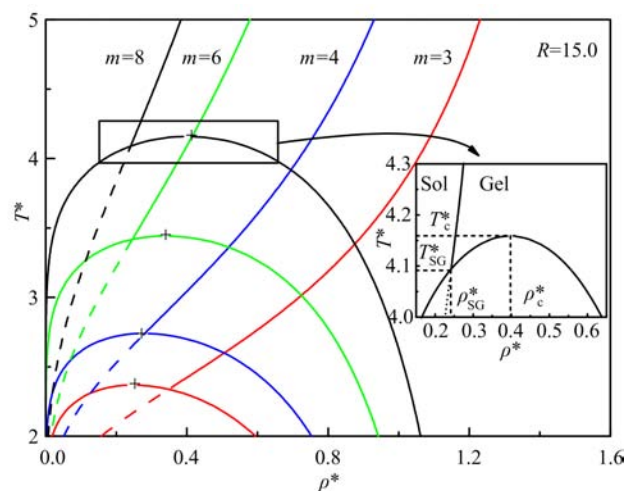


FIG. 8  $T^*$ - $\rho^*$  phase diagrams of the SGT and F-F transition in  $A_m$  type of patchy system at  $R=15.0$  for  $m=3, 4, 6$ , and  $8$ , where the solid lines above the binodal curves are the corresponding SGT lines. The insert denotes the local diagram at  $m=8$  and  $R=15.0$ , which is to interpret the critical point ( $\rho_c^*, T_c^*$ ) and the intersection ( $\rho_{SG}^*, T_{SG}^*$ ).

association energy plays a key role in determining if a gel phase can be considered to be a glassy state.

At a low association energy, the lifetime of colloidal clusters just above  $p_c$  is still limited so that the gel density may meet the conditions of the glassy state. For patchy particles under this condition, its gel phase can not discriminate itself from its glassy state, thereby becoming equivalent to a glassy state. However, at a high association energy, it is possible that there is a large density difference between the gel phase and the glassy state. In this situation, the development of the system from a gel phase to a glassy state needs some extra effort such as quenching, changing the solvent quality, increasing the associated fraction  $p$ , and so forth. As a result, the interplay between the gel phase and glassy state is very subtle, so do the SGT, F-F, and the F-RCP transitions.

## V. CONCLUSION

To summarize, the phase diagrams of  $A_m$  type of patchy colloidal particles have been presented, in which F-F, F-RCP, and F-FCC transitions together with SGT are illustrated. An attempt is made to elucidate the effect of the interparticle associating interaction on the phase equilibria of patchy particles. In our treatment, the RCP phase with the density of maximum packing ( $\rho_{cp}^{RCP*}=1.203$ ) has been used as the critical glassy state. This is due to the fact that the glassy state is stable with respect to a fluid only when  $0.943 < \rho^* < 1.203$ . On the basis of this point, the F-RCP transition is studied by the standard theory for thermodynamic phase transitions. Namely, we are considering the RCP phase as

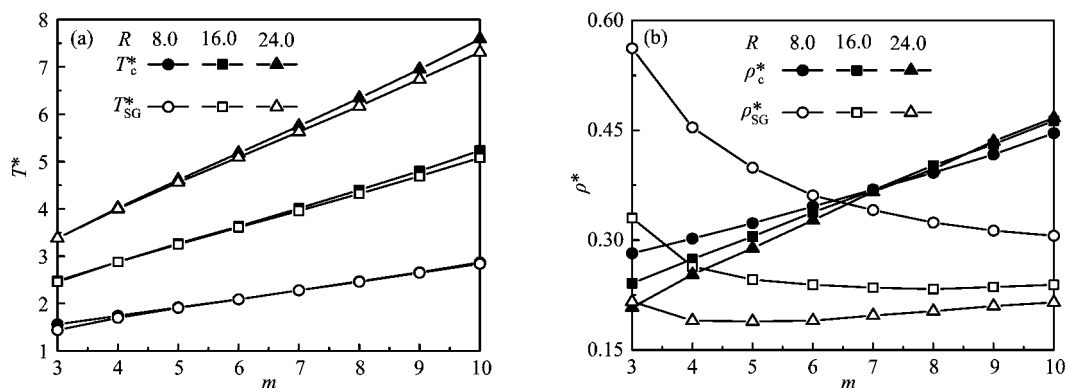


FIG. 9 Plots of  $T_{SG}^*$  and  $T_c^*$  (a), and  $\rho_{SG}^*$  and  $\rho_c^*$  (b) against  $m$  for  $A_m$  type of patchy system.

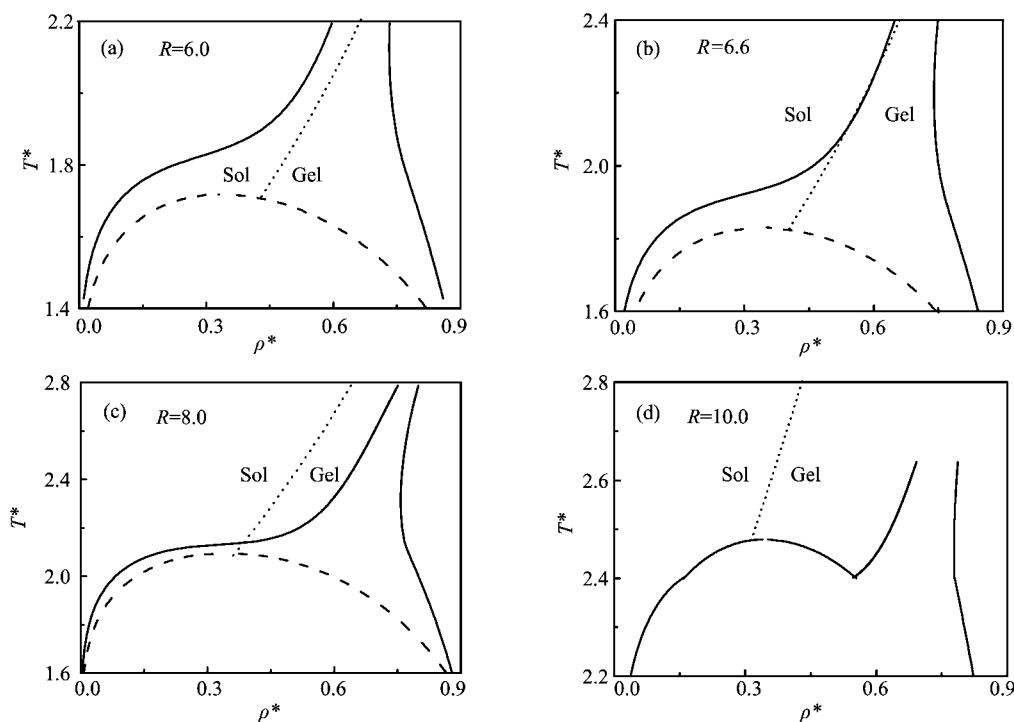


FIG. 10  $T^*$ - $\rho^*$  phase diagrams of the SGT (short dot line), F-F (dash line), and F-RCP (solid line) transitions in  $A_6$  type of patchy system at different  $R$ : (a)  $R=6.0$ , (b)  $R=6.6$ , (c)  $R=8.0$ , (d)  $R=10.0$ .

a pseudo-thermodynamic phase. Such a treatment is merely to capture qualitatively some common features on the glass transition of patchy particles.

As a matter of fact, the associating interaction between two patchy particles is jointly determined by the association energy and valence (the number of patches). As expected, the phase behavior of the system shows a significant dependence on these factors. Several main findings are as follows: (i) the critical temperature  $T_c^*$ , and triple points temperature ( $T_{tp(FCC)}^*$  and  $T_{tp(RCP)}^*$ ) increase with the association energy and valence; (ii) whether the liquid-like fluid is metastable or stable with respect to RCP or FCC phases depends strongly on the associating interaction between patchy

particles; (iii) a smaller valence allows larger temperature and density ranges to form an equilibrium gel of patchy particles. More importantly, under what conditions and to what extent the gel phase can be identified as a glassy state are also closely related to the association energy and valence; (iv) in view of the changeable valence and association energy of patchy particles, the present patchy system can, in principle, serve as a model system to illustrate two types of possible mechanisms for nucleation in crystallization.

From these results, one can conclude that the control of the associating interaction between two patchy particles provides an effective way of regulating aggregated state and phase structures of patchy particles.

Note that several approximations have been made in the present study because some practical systems of patchy colloidal particles are indeed very complicated. First, the model of spherical colloidal particles is used, which ignores the anisotropy due to non-spherical structure of some patchy particles. Second, the anisotropy due to the different valences of patchy particles is replaced by an averaged associating potential. It is evident that the anisotropy will affect the self-assembly of patchy particles, which is different from the present treatment based on the mean-field model. Third, the influence of the loop structures in colloidal clusters is also ignored. The loop structures not only contribute to the association free energy, but also give rise to a delay of the gel point. Thus, some further investigations by relaxing these approximations are noteworthy, and the relevant efforts are underway.

## VI. ACKNOWLEDGMENTS

This work was supported by the National Natural Science Foundation of China (No.21374028 and No.21306034), the Natural Science Foundation of Hebei Province (No.B2014201103), the Project for Talent Engineering of Hebei Province (No.A2016015001), the Project for Top Young Talent of Hebei Province, and the Project for Top Young Talent of General Colleges of Hebei Province (No.BJ2017017).

- [1] M. Sabapathy, S. D. C. Pushpam, M. G. Basavaraj, and E. Mani, *Langmuir* **31**, 1255 (2015).
- [2] S. H. Kim, A. Abbaspourrad, and D. A. Weitz, *J. Am. Chem. Soc.* **133**, 5516 (2011).
- [3] J. He, M. J. Hourwitz, Y. J. Liu, M. T. Perez, and Z. H. Nie, *Chem. Commun.* **47**, 12450 (2011).
- [4] Y. H. Wang, C. L. Zhang, C. Tang, J. Li, K. Shen, J. G. Liu, X. Z. Qu, J. L. Li, Q. Wang, and Z. Z. Yang, *Macromolecules* **44**, 3787 (2011).
- [5] L. L. Ge, J. J. Li, S. T. Zhong, Y. Sun, S. E. Friberg, and R. Guo, *Soft Matter* **13**, 1012 (2017).
- [6] Z. F. Cheng, F. H. Luo, Z. X. Zhang, and Y. Q. Ma, *Soft Matter* **9**, 11392 (2013).
- [7] K. H. Roh, D. C. Martin, and J. Lahann, *Nat. Mater.* **4**, 759 (2005).
- [8] A. Walther and A. H. E. Müller, *Soft Matter* **4**, 663 (2008).
- [9] K. Chaudhary, Q. Chen, J. J. Juárez, S. Granick, and J. A. Lewis, *J. Am. Chem. Soc.* **134**, 12901 (2012).
- [10] A. A. Shah, B. Schultz, K. L. Kohlstedt, S. C. Glotzer, and M. J. Solomon, *Langmuir* **29**, 4688 (2013).
- [11] B. Fang, A. Walther, A. Wolf, Y. Y. Xu, J. Y. Yuan, and A. H. E. Müller, *Angew. Chem. Int. Ed.* **48**, 2877 (2009).
- [12] Y. F. Wang, Y. Wang, D. R. Breed, V. N. Manoharan, L. Feng, A. D. Hollingsworth, M. Weck, and D. J. Pine, *Nature* **491**, 51 (2012).
- [13] C. De Micheleand, S. Gabrielli, P. Tartaglia, and F. Sciortino, *J. Phys. Chem. B* **110**, 8064 (2006).
- [14] A. Giacometti, F. Lado, J. Largo, G. Pastore, and F. Sciortino, *J. Chem. Phys.* **132**, 174110 (2010).
- [15] M. G. Noro, N. Kern, and D. Frenkel, *Europhys. Lett.* **9**, 332 (1999).
- [16] J. P. K. Doye, A. A. Louis, I. C. Lin, L. R. Allen, E. G. Noya, A. W. Wilber, H. C. Kok, and R. Lyus, *Phys. Chem. Chem. Phys.* **9**, 2197 (2007).
- [17] C. J. Roberts and M. A. Blanco, *J. Phys. Chem. B* **118**, 12599 (2014).
- [18] Z. Zhang and S. C. Glotzer, *Nano. Lett.* **4**, 1407 (2004).
- [19] A. B. Pawar, I. Kretzschmar, G. Aranovich, and M. D. Donohue, *J. Phys. Chem. B* **111**, 2081 (2007).
- [20] A. W. Wilber, J. P. K. Doye, A. A. Louis, E. G. Noya, M. A. Miller, and P. Wong, *J. Chem. Phys.* **127**, 085106 (2007).
- [21] B. Capone, I. Coluzza, R. Blaak, F. Lo Verso, and C. N. Likos, *New J. Phys.* **15**, 095002 (2013).
- [22] F. Smalenburg, L. Filion, and F. Sciortino, *Nat. Phys.* **10**, 653 (2014).
- [23] E. G. Noya and E. Bianchi, *J. Phys. Condens. Matter* **27**, 234103 (2015).
- [24] Z. W. Li, Z. Y. Lu, Y. L. Zhu, Z. Y. Sun, and L. J. An, *RSC. Adv.* **3**, 813 (2013).
- [25] Q. Z. Zou, Z. W. Li, Z. Y. Lu, and Z. Y. Sun, *Nanoscale* **8**, 4070 (2016).
- [26] J. M. Tavares, N. G. Almarza, and M. M. T. da Gama, *J. Chem. Phys.* **140**, 044905 (2014).
- [27] I. Saika-Voivod, F. Smalenburg, and F. Sciortino, *J. Chem. Phys.* **139**, 234901 (2013).
- [28] A. Reinhardt, F. Romano, and J. P. K. Doye, *Phys. Rev. Lett.* **110**, 255503 (2013).
- [29] X. M. Mao, Q. Chen, and S. Granick, *Nat. Mater.* **12**, 217 (2013).
- [30] D. Paloli, P. S. Mohanty, J. J. Crassous, E. Zaccarelli, and P. Schurtenberger, *Soft Matter* **9**, 3000 (2013).
- [31] F. Sciortino and E. Zaccarelli, *Curr. Opin. Solid State Mat. Sci.* **15**, 246 (2011).
- [32] F. Sciortino and E. Zaccarelli, *Curr. Opin. Colloid Interface Sci.* **30**, 90 (2017).
- [33] F. Sciortino, *Eur. Phys. J. B* **64**, 505 (2008).
- [34] J. Russo, P. Tartaglia, and F. Sciortino, *J. Chem. Phys.* **131**, 014504 (2009).
- [35] F. Romano, P. Tartaglia, and F. Sciortino, *J. Phys. Condens. Matter*, **19**, 322101 (2007).
- [36] H. Liu, S. K. Kumar, F. Sciortino, and G. T. Evans, *J. Chem. Phys.* **130**, 044902 (2009).
- [37] J. M. Tavares, P. I. C. Teixeira, and M. M. Telo da Gama, *Phys. Rev. E* **80**, 021506 (2009).
- [38] X. Z. Hong, F. Gu, J. T. Li, and H. J. Wang, *Chem. J. Chin. Univ.* **35**, 1579 (2014).
- [39] J. L. Finney and L. V. Woodcock, *J. Phys.: Condens. Matter*, **26**, 463102 (2014).
- [40] G. Parisi and F. Zamponi, *Rev. Mod. Phys.* **82**, 789 (2010).
- [41] P. Charbonneau, A. Ikeda, G. Parisi, and F. Zamponi, *Phys. Rev. Lett.* **107**, 185702 (2011).
- [42] M. Baus and C. F. Tejero, *Equilibrium Statistical Physics: Phases of Matter and Phase Transitions*, Germany: Springer, 192 (2007).
- [43] R. Angelini, E. Zaccarelli, F. A. D. Marques, M. Sztucki, A. Fluerasu, G. Ruocco, and B. Ruzicka, *Nat.*

- Commun. **5**, 4049 (2014).
- [44] C. Valeriani, E. Sanz, E. Zaccarelli, W. C. K. Poon, M. E. Cates, and P. N. Pusey, *J. Phys.: Condens. Matter*, **23**, 194117 (2011).
- [45] S. Roldan-Vargas, L. Rovigatti, and F. Sciortino, *Soft Matter*, **13**, 514 (2017).
- [46] C. Mondal, S. Karmakar, and S. Sengupta, *J. Phys. Chem. B* **119**, 10902 (2015).
- [47] N. Kern and D. Frenkel, *J. Chem. Phys.* **118**, 9882 (2003).
- [48] M. S. Wertheim, *J. Chem. Phys.* **85**, 2929 (1986).
- [49] L. Y. Wang, F. Gu, H. J. Wang, and Z. L. Sun, *J. Phys. Chem. B* **121**, 2142 (2017).
- [50] E. Bianchi, J. Largo, P. Tartaglia, E. Zaccarelli, and F. Sciortino, *Phys. Rev. Lett.* **97**, 168301 (2006).
- [51] E. Bianchi, P. Tartaglia, E. Zaccarelli, and F. Sciortino, *J. Chem. Phys.* **128**, 144504 (2008).
- [52] M. S. Wertheim, *J. Stat. Phys.* **35**, 19 (1984).
- [53] N. F. Carnahan and K. E. Starling, *J. Chem. Phys.* **51**, 635 (1969).
- [54] P. Tartaglia and F. Sciortino, *J. Phys. Condens. Matter*, **22**, 104108 (2010).
- [55] F. Sciortino, E. Bianchi, J. F. Douglas, and P. Tartaglia, *J. Chem. Phys.* **126**, 194903 (2007).
- [56] N. W. Ashcroft and N. D. Mermin, *Solid State Physics*, Orlando: Harcourt, 400 (1976).
- [57] F. Smallenburg, L. Leibler, and F. Sciortino, *Phys. Rev. Lett.* **111**, 188002 (2013).
- [58] E. Zaccarelli, F. Sciortino, and P. Tartaglia, *J. Phys.: Condens. Matter* **16**, S4849 (2004).
- [59] E. Zaccarelli, *J. Phys. Condens. Matter* **19**, 323101 (2007).
- [60] E. Zaccarelli, F. Sciortino, P. Tartaglia, G. Foffic, G. D. McCullagh, A. Lawlor, and K. A. Dawson, *Physica A* **314**, 539 (2002).
- [61] G. Foffi, K. A. Dawson, S. V. Buldyrev, F. Sciortino, E. Zaccarelli, and P. Tartaglia, *Phys. Rev. E* **65**, 050802 (2002).
- [62] F. Krzakala, M. Tarzia, and L. Zdeborová, *Phys. Rev. Lett.* **101**, 165702 (2008).
- [63] P. R. Ten Wolde and D. Frenkel, *Science* **277**, 1975 (1997).
- [64] V. Talanquer and D. W. Oxtoby, *J. Chem. Phys.* **109**, 223 (1998).
- [65] J. F. Lutsko and G. Nicolis, *Phys. Rev. Lett.* **96**, 046102 (2006).
- [66] T. H. Zhang and X. Y. Liu, *J. Am. Chem. Soc.* **129**, 13520 (2007).
- [67] D. Erdemir, A. Y. Lee, and A. S. Myerson, *Accounts. Chem. Res.* **42**, 621 (2009).
- [68] M. Rubinstein and R. H. Colby, *Polymer Physics*, Oxford: Oxford University Press, 206 (2003).